Kent Academic Repository Full text document (pdf)

Citation for published version

Schneider, Constanze and Oellerich, Thomas and Baldauf, Hanna-Mari and Schwarz, Sarah-Marie and Thomas, Dominique and Flick, Robert and Bohnenberger, Hanibal and Kaderali, Lars and Stegmann, Lena and Cremer, Anjali and Martin, Margarethe and Lohmeyer, Julian and Michaelis, Martin and Hornung, Veit and Schliemann, Christoph and Berdel, Wolfgang E and Hartmann,

DOI

https://doi.org/10.1038/nm.4255

Link to record in KAR

http://kar.kent.ac.uk/60380/

Document Version

Author's Accepted Manuscript

Copyright & reuse

Content in the Kent Academic Repository is made available for research purposes. Unless otherwise stated all content is protected by copyright and in the absence of an open licence (eg Creative Commons), permissions for further reuse of content should be sought from the publisher, author or other copyright holder.

Versions of research

The version in the Kent Academic Repository may differ from the final published version. Users are advised to check http://kar.kent.ac.uk for the status of the paper. Users should always cite the published version of record.

Enquiries

For any further enquiries regarding the licence status of this document, please contact: **researchsupport@kent.ac.uk**

If you believe this document infringes copyright then please contact the KAR admin team with the take-down information provided at http://kar.kent.ac.uk/contact.html





1 SAMHD1 is a biomarker for cytarabine response and a therapeutic target

2 in acute myeloid leukemia

- 3 Constanze Schneider^{1,§}, Thomas Oellerich^{2,3,4,§}, Hanna-Mari Baldauf^{1,5§}, Sarah-Marie
- 4 Schwarz^{1,§}, Dominique Thomas⁶, Robert Flick⁷, Hanibal Bohnenberger⁸, Lars Kaderali⁹, Lena
- 5 Stegmann¹, Anjali Cremer³, Margarethe Martin¹, Julian Lohmeyer³, Martin Michaelis¹⁰, Veit
- 6 Hornung^{11,12}, Christoph Schliemann¹³, Wolfgang E. Berdel¹³, Wolfgang Hartmann¹⁴, Eva
- 7 Wardelmann¹⁴, Federico Comoglio³, Martin-Leo Hansmann¹⁵, Alexander F. Yakunin⁷, Gerd
- 8 Geisslinger^{6,16}, Philipp Ströbel⁸, Nerea Ferreirós⁶, Hubert Serve^{2,4,*}, Oliver T. Keppler^{1,5,**} &
- 9 Jindrich Cinatl Jr.^{1,**}
- 10

¹Institute of Medical Virology, University of Frankfurt, Frankfurt, Germany, ²Department of Medicine II, Hematology/Oncology, Goethe University of Frankfurt, Frankfurt, Germany. ³Cambridge University Department of Haematology, Cambridge Institute of Medical Research, Cambridge, United Kingdom, ⁴German Cancer Consortium/ German Cancer Research Center, Heidelberg, Germany. ⁵Max von Pettenkofer-Institute, Department of Virology, Ludwig Maximilian University of Munich, Munich, Germany. ⁶pharmazentrum frankfurt/ZAFES, Institute of Clinical Pharmacology, Goethe University of Frankfurt, Frankfurt, Germany. ⁷Department of Chemical Engineering and Applied Chemistry, University of Toronto, Toronto, Ontario, Canada. ⁸Institute of Pathology, University Medical Center, Göttingen, Germany. ⁹Institute of Bioinformatics, University Medicine Greifswald, Greifswald, Germany.¹⁰Centre for Molecular Processing and School of Biosciences, University of Kent, Canterbury United Kingdom.¹¹Institute of Molecular Medicine, University Hospital Bonn, Bonn, Germany.¹²Gene Center and Department of Biochemistry, Ludwig Maximilian University of Munich, Munich, Germany.¹³Department of Medicine A (Hematology, Oncology), University Hospital Münster, Germany.¹⁴Gerhard Domagk Institute for Pathology, University Hospital Münster, Germany.¹⁵Senckenberg Institute of Pathology, University of Frankfurt, Frankfurt, Germany.¹⁶Fraunhofer Institute for Molecular Biology and Applied Ecology (IME), Project group Translational Medicine and Pharmacology (TMP), Frankfurt, Germany.

- 11
- 12 [§]C.S., T.O., H.-M.B. and S.-M.S. contributed equally
- 13 *Co-correspondence for clinical studies: H.S. (Hubert.Serve@kgu.de)
- 14 **Senior co-correspondence: O.T.K. (keppler@mvp.uni-muenchen.de) or J.C.
- 15 (Cinatl@em.uni-frankfurt.de)

16 The nucleoside analog cytarabine (Ara-C) is an essential component of primary and 17 salvage chemotherapy regimens in acute myeloid leukemia (AML). After cellular 18 uptake, Ara-C is converted into its therapeutically active triphosphate metabolite, Ara-19 CTP, which exerts anti-leukemic effects primarily by inhibiting DNA synthesis in proliferating cells¹. Currently, a substantial fraction of AML patients fails to effectively 20 respond to Ara-C therapy and reliable biomarkers are lacking^{2,3}. SAMHD1 is a 21 22 deoxynucleoside triphosphate (dNTP) triphosphohydrolase that cleaves physiological dNTPs into deoxyribonucleosides and inorganic triphosphate^{4,5}. Although it has been 23 24 postulated that SAMHD1 sensitizes cancer cells to nucleoside analog derivatives through depletion of competing dNTPs⁶, we show here that SAMHD1 reduces Ara-C cytotoxicity 25 26 in AML cells. Mechanistically, dGTP-activated SAMHD1 hydrolyzes Ara-CTP, 27 resulting in a drastic reduction of Ara-CTP in leukemic cells. Loss of SAMHD1 activity -28 through genetic depletion, mutational inactivation of its triphosphohydrolase activity, or proteasomal degradation using specialized virus-like particles^{7,8} - potentiates the 29 30 cytotoxicity of Ara-C in AML cells. In mouse retroviral AML transplantation models as 31 well as in retrospective analyses of adult AML patients, the response to Ara-C-32 containing therapy was inversely correlated with SAMHD1 expression. These results 33 identify SAMHD1 as a potential biomarker for the stratification of AML patients to 34 Ara-C-based therapy and as a target for treating Ara-C-refractory AML.

35

37 The current backbone of AML therapy is treatment with the cytidine analog Ara-C and the 38 anthracycline daunorubicin. Despite a high rate of initial remissions, a substantial fraction of AML patients relapses and acquires resistance to Ara-C^{1,9}. The prognosis of AML patients, 39 especially elderly ones, remains dismal^{2,9}. Mutations in the SAMHD1 gene, encoding Sterile 40 41 alpha motif and histidine-aspartic domain-containing protein 1 (SAMHD1), have been associated with the Aicardi-Goutières autoimmune syndrome¹⁰ and the development of 42 43 malignancies including cutaneous T-cell lymphoma, chronic lymphatic leukemia, and colon cancer¹¹⁻¹³. 44 SAMHD1, a dNTP triphosphohydrolase that cleaves dNTPs into 45 deoxyribonucleosides and inorganic triphosphate, enhances the efficacy of certain nucleoside 46 analog drugs for the treatment of human immunodeficiency virus type-1 (HIV-1) by decreasing the levels of intracellular dNTPs^{14,15}, which apparently compete with the 47 thymidine analog triphosphates for incorporation into HIV-1 cDNA during reverse 48 transcription¹⁶. We postulated that SAMHD1 could have a similar effect on nucleoside 49 analog-based therapy in leukemia⁶. 50

51 To investigate whether SAMHD1 expression enhances Ara-C cytotoxicity in AML 52 cells, we tested whether Ara-C sensitivity in 13 AML cell lines, determined by the half 53 maximal inhibitory concentration (IC₅₀), is correlated with SAMHD1 protein and mRNA 54 levels. Both SAMHD1 expression (Fig. 1a and Supplementary Fig. 1) and Ara-C sensitivity 55 (Supplementary Table 1) varied considerably among these cell lines. Unexpectedly, 56 SAMHD1 levels inversely correlated with Ara-C cytotoxicity (p=0.0037, Fig. 1b and 57 Supplementary Fig. 2a,b), as well as with the levels of early (Caspase 3 and 7 activity, 58 p=0.02, Supplementary Fig. 3a,b) and late (sub-G1 cells, apoptotic DNA fragmentation, 59 p=0.029, Supplementary Fig. 3c,d) markers of apoptosis. In contrast, no significant 60 correlation could be established between Ara-C IC₅₀ values and the expression of cellular proteins previously implicated in Ara-C uptake or its conversion to Ara-CTP¹, including
equilibrative nucleoside transporter (ENT1/SLC29A1), deoxycytidine kinase (DCK), cytidine
deaminase (CDA), deoxycytidilate deaminase (DCTD), or 5'-nucleotidase (NT5C2) (Fig.
1a,c-g).

65 To further investigate its role in Ara-C resistance, we tested the effects of SAMHD1 66 deficiency by a number of approaches: (i) depletion of SAMHD1 in AML cell lines 67 expressing high endogenous SAMHD1 levels using either lentiviral vectors encoding 68 SAMHD1-specific shRNA or transfection with SAMHD1-specific siRNA; (ii) CRISPR/Cas9-69 mediated disruption of the SAMHD1 gene; and (iii) targeted degradation of SAMHD1 using 70 virus-like particles (VLPs) which shuttle the SAMHD1-interacting lentiviral Vpx protein (Vpx-VLPs) into cells^{7,8,17} (Fig. 2a and Supplementary Fig. 4). Vpx recruits SAMHD1 to a 71 cullin4A-RING E3 ubiquitin ligase (CRL4^{DCAF1}), which targets the enzyme for proteasomal 72 degradation^{7,8}. 73

74 SAMHD1 depletion in AML cell lines by RNA interference (OCI-AML3, THP-1), SAMHD1 knockout (THP-1^{-/-}), or transduction with Vpx-VLPs (MonoMac6 cells, THP-1) 75 76 markedly sensitized AML cell lines to Ara-C toxicity relative to the respective controls (Fig. 77 **2a,b** and **Supplementary Fig. 4**). In contrast, *SAMHD1* siRNA had only a marginal effect on 78 Ara-C toxicity in low SAMHD1-expressing HEL cells (Fig. 2a,b). Interestingly, we observed 79 SAMHD1 dependency, although less pronounced, for the purine analog fludarabine 80 (Supplementary Fig. 5a); however, the IC_{50} values for the topoisomerase II inhibitors 81 etoposide and daunorubicin, as well as for dFdC (2',2'-difluorodeoxycytidine; gemcitabine), 82 were not consistently affected by SAMHD1 down-modulation (Supplementary Fig. 5b-d), 83 indicating a certain degree of drug specificity.

84 In HEL cells, an AML cell line that expresses very low endogenous levels of 85 SAMHD1 (Fig. 1a and Fig. 2a,c), constitutive overexpression of wild-type SAMHD1 (SAMHD1-WT), but not of the dNTPase-deficient SAMHD1-D311A mutant, increased the 86 87 IC₅₀ values for Ara-C and fludarabine (Fig. 2c and Supplementary Fig. 5a). In contrast, the 88 toxicity of daunorubicin, etoposide, or dFdC was largely unaltered (Supplementary Fig. 5b-89 d). These results indicate that SAMHD1's enzymatic activity is critically involved in 90 mediating resistance of AML cells to Ara-C and, to a lesser extent, fludarabine. Notably, Ara-91 C at concentrations mimicking the steady state levels of Ara-C in plasma during standard Ara-C regimens $(100-200 \text{ mg/m}^2)^1$ or the minimum blood plasma concentration (C_{min}; achieved 92 12h after completion of i.v. infusion) during high-dose Ara-C therapy $(3000 \text{ mg/m}^2)^{18}$ only 93 94 partially affected the viability of SAMHD1-expressing AML cell lines, whereas SAMHD1-95 depleted cells were effectively killed (Supplementary Fig. 6).

96 Although previous in vitro studies provided no evidence that triphosphorylated antiviral nucleoside analogs can be hydrolyzed by SAMHD1^{19,20}, we hypothesized that SAMHD1 97 98 might be able to hydrolyze Ara-CTP, which differs from the physiological dCTP substrate by 99 only a hydroxyl substituent in the up-position at carbon atom-2 of the pentose moiety 100 (Supplementary Fig. 7). To directly test whether Ara-CTP is hydrolyzed by SAMHD1, we 101 quantified Ara-CTP levels relative to SAMHD1 expression following short-term exposure of AML cells to ¹³C₃-Ara-C, using liquid chromatography tandem mass spectrometry (LC-102 MS/MS). We detected 47-fold higher Ara-CTP levels in SAMHD1-deficient THP-1^{-/-} cells 103 compared to THP-1^{+/+} control cells (Supplementary Fig. 8a), whereas SAMHD1 deficiency 104 105 did not affect dFd-CTP levels after drug treatment (Supplementary Fig. 8b). Moreover, HEL 106 SAMHD1-WT cells harbored 97- and 69-fold lower levels of Ara-CTP compared to parental 107 HEL cells and HEL cells expressing the SAMHD1-D311A mutant, respectively (Fig. 2d).

108 Notably, lack of enzymatically active SAMHD1 in THP-1^{-/-} cells or in parental and 109 SAMHD1-D311A-expressing HEL cells also resulted in elevated dNTP levels 110 (**Supplementary Fig. 9a,b**), which, however, did not counteract the cytotoxicity of the 111 concomitantly increased Ara-CTP levels (**Fig. 2b,c**).

112 dGTP or GTP binding to the primary allosteric site of SAMHD1 leads to formation of 113 a catalytically active tetramer, whereas the second allosteric site of the enzyme accommodates dNTPs²¹⁻²³. To elucidate whether Ara-CTP can serve as a substrate or as both an activator and 114 115 substrate for the triphosphohydrolase, we performed an enzymatic in vitro assay using 116 bacterially expressed full-length SAMHD1. Analysis of reaction products by ion-pair reverse-117 phase HPLC revealed that SAMHD1 hydrolyzes Ara-CTP to Ara-C, requiring the presence of 118 the activator dGTP, which itself is also cleaved to dG (Fig. 2e). In specificity control 119 experiments, the physiological substrate TTP, but not dFd-CTP, was hydrolyzed by SAMHD1 120 (Supplementary Fig. 10a,b). Thus, Ara-CTP is a direct substrate, but not an activator, of 121 SAMHD1's triphosphohydrolase activity in AML cells.

122 To explore whether SAMHD1 might contribute to the development of Ara-C 123 resistance, we gradually adapted three AML cell lines (HEL, HL-60, and Molm13), 124 characterized by low endogenous SAMHD1 expression levels and high Ara-C sensitivity, to 125 growth in the presence of the nucleoside analog. The resulting drug-resistant sublines were cultivated in medium containing Ara-C at a concentration of 2 µg/ml (designated ^rAra-C^{2µg}) 126 and displayed increases in Ara-C IC₅₀ values ranging from 1643- to 4250-fold relative to the 127 128 parental cell lines (Supplementary Table 2). In addition to changes in the expression of some 129 cellular factors previously implicated in acquired Ara-C resistance (i.e., DCK, CDA, and 130 NT5C2), the levels of SAMHD1 were markedly increased in the Ara-C-resistant sublines 131 relative to their parental counterparts (Fig. 3a and Supplementary Fig. 11). Ara-C resistance was accompanied by drastically decreased Ara-CTP levels (Fig. 3b) and exposure of Ara-Cresistant AML cells to Vpx-VLPs depleted SAMHD1, increased Ara-CTP levels, and resensitized the cells to Ara-C by up to 11.5-fold relative to Vpr-VLP-treated control cells (Fig.
3c,d). Whereas cultivation of the parental AML cell lines in the presence of the drug for 24 h
did not acutely induce SAMHD1 levels (Supplementary Fig. 12a), selection for 20 d in
Molm13 cells resulted in an upregulation of SAMHD1 levels (Supplementary Fig. 12b).

138 To study the role of SAMHD1 in AML drug sensitivity *in vivo*, we transformed mouse 139 myeloid progenitor cells using the oncogenes Hoxa9/Meis1 or MN1 and subsequently deleted 140 the SAMHD1 gene using CRISPR/Cas9 genome editing with two independent guide RNAs (gRNA). SAMHD1^{+/+} control AML blasts and knockout (SAMHD1^{-/-}) AML blasts were 141 142 transplanted into irradiated recipient mice, and were treated with either Ara-C or phosphate-143 buffered saline (PBS) on day 18 and 19 after transplantation (Supplementary Fig. 13a-d). Overall survival of the two independent mouse cohorts transplanted with SAMHD1-/- AML 144 was dramatically prolonged compared to SAMHD1^{+/+} AML by administration of Ara-C (Fig. 145 4a,b $(p=2.97 \times 10^{-6} \text{ for both cohorts})$, Supplementary Fig. 13e $(p=3.05 \times 10^{-6})$ and 146 Supplementary Fig. 13f (p=4.32x10⁻⁶)), but not by PBS treatment (Fig. 4a,b and 147 148 Supplementary Fig. 13e,f). Similar results were obtained for two mouse cohorts for which a 149 second SAMHD1 gRNA was used (Supplementary Fig. 14).

In human blasts isolated from bone marrow of therapy-naïve AML patients, basal SAMHD1 expression correlated with Ara-C IC_{50} values (p=0.04, **Supplementary Fig. 15**). Moreover, we tested the effects of transient depletion of SAMHD1 in blasts of six patients (**Supplementary Table 3**, patients A to F). Two days after transfection with control or *SAMHD1*-targeting siRNA, the blasts were cultured in the presence of Ara-C or daunorubicin. SAMHD1 depletion diminished Ara-C IC_{50} values by 3- to 15-fold (**Fig. 4c**), whereas the 156 sensitivity of the blasts to daunorubicin was unaltered (Supplementary Table 4). Similarly, 157 treatment with SAMHD1-degrading Vpx-VLPs sensitized primary AML blasts to Ara-C, but 158 not to daunorubicin, compared to Vpr-containing control VLPs (Supplementary Fig. 16 and 159 **Supplementary Table 5**). Concomitantly with this sensitization, intracellular Ara-CTP levels 160 were elevated (Supplementary Fig. 8c,d). Finally, we examined the suitability of SAMHD1 161 expression as a biomarker for predicting the response of AML to standard Ara-C-containing 162 therapy. We analyzed an AML cohort of 150 adult patients who had received one to two 163 courses of Ara-C-containing induction therapy in two University Hospital study centers in Germany. Patients received either two cycles of "7+3" or "7+3" plus high-dose Ara-C in 164 165 combination with mitoxantrone (HAM) according to standard German AML protocols 166 (Supplementary Table 6). The "7+3" treatment regime refers to 7 days of standard-dose 167 Ara-C with the addition of daunorubicin for 3 days during the 7 day-chemotherapy induction 168 cycle (see Online Methods). Retrospective analysis of SAMHD1 protein levels by 169 immunohistochemical (IHC) staining of blasts in sections of paraffinized bone marrow 170 isolated at primary diagnosis revealed that expression of SAMHD1 was highly variable 171 between patients and, importantly, markedly increased in the group of AML patients that did 172 not reach a complete remission ("No CR", n=38) at the end of induction therapy, as compared to the group of patients with documented complete remission ("CR", n=112) ($p=6.3 \times 10^{-8}$, 173 174 Wilcoxon Rank Sum test) (Fig. 4d,e and Supplementary Table 6). Of the 150 patients, 112 175 achieved CR; of these 90 were scored as "SAMHD1-low" and 22 were scored as "SAMHD1-176 high". The CR rate in the "SAMHD1-high" cohort was 22/50 (44%), whereas the CR rate in 177 the "SAMHD1-low" cohort was 90/100 (90%). This difference between the two SAMHD1stratified cohorts was highly statistically significant $(p=3.477 \times 10^{-9})$. Chi-Squared Test 178 179 with 1 degree of freedom). As a validation of the IHC staining and scoring system, levels of

180 SAMHD1 protein expression in blasts as determined by IHC scoring and in parallel by flow 181 cytometry showed a positive correlation (p<0.0001, Supplementary Fig. 17b). All CR 182 patients received post-remission therapy: a high-dose Ara-C-containing chemo-consolidation 183 regimen and/or allogeneic stem cell transplantation. In our AML cohort, the level of 184 SAMHD1 expression in blasts at initial diagnosis was highly predictive for event-free survival (EFS) ($p=1.86 \times 10^{-11}$, Fig. 4f), where an event was defined as failure to achieve CR. 185 186 relapse or death. Also, relapse-free survival (RFS) of CR patients was significantly worse in "SAMHD1-high" compared to "SAMHD1-low" patients (p=2.02 x10⁻⁴, Fig. 4g), indicating 187 188 that the depth of remission in "SAMHD1-high" patients was less pronounced than in "SAMHD1-low" patients. Although the median observation time was relatively short, 189 190 "SAMHD1-high" patients experienced a significantly worse overall survival (OS) (p=4.85 $x10^{-3}$, Fig. 4h). When patients were censored from the analyses at the time of allogeneic 191 192 transplantation, all differences (EFS, RFS, OS) remained statistically significant 193 (Supplementary Fig. 18a-c). Notably, no correlation could be established between 194 cytogenetic risk groups and SAMHD1 expression (Supplementary Fig. 19a). In a 195 multivariate analysis including age, gender, initial leukocyte count and cytogenetic risk group, and type of second induction cycle (HAM versus "7+3"), high SAMHD1 expression proved 196 to be an independent risk factor for EFS (hazard ratio 1.72, p= 5.23×10^{-8}) and OS (1.33, 197 198 p=0.0228) (Supplementary Fig. 19b,c).

Furthermore, mining of the publicly available AML data set of the TCGA cohort²⁴ confirmed a correlation between low SAMHD1 mRNA expression with CR for patients who had received an Ara-C-containing therapy (**Supplementary Fig. 20**). Thus, SAMHD1 levels at diagnosis inversely correlate with the clinical response to Ara-C-based therapy in two different adult AML patient cohorts, and this prominent role of SAMHD1 in Ara-C responseis corroborated by results from murine AML transplantation models.

205 Taken together, this study identifies SAMHD1 as a cellular biomarker for stratification 206 of patients to Ara-C-based therapy and uncovers a patient- and drug-specific interference 207 mechanism (Supplementary Fig. 21) that, in addition to established molecular and cytogenetic risk factors²⁵, determines the outcome of AML disease. Ara-C's mimicry of the 208 209 physiological nucleoside cytidine endows it with anti-leukemic activity, but this mimicry is 210 detrimental in AML blasts that express the Ara-CTP-inactivating SAMHD1 protein. This 211 concept applies to a lesser extent also to the purine analog fludarabine, but not to dFdC, 212 indicating that SAMHD1 should be considered a critical cellular factor in the evaluation of all 213 nucleoside analog-based drugs or drug candidates in AML. Future studies will determine 214 whether protein- or mRNA-based quantification of SAMHD1 in AML blasts at diagnosis is a 215 better predictor of the therapeutic response. In vivo strategies aiming at transient 216 downregulation of SAMHD1 by either RNA interference or application of SAMHD1-217 degrading Vpx-VLPs, or, conceivably, through administration of an inhibitor of SAMHD1's 218 enzymatic activity, may improve the Ara-C-based treatment of AML and other malignancies.

219

220 METHODS

221 Methods and any associated reference are available in the online version of the paper.

Note: Any Supplementary Information and Source Data files are available in the onlineversion of the paper.

224

225 Acknowledgements

226 This study to dedicated to the memory of Prof. Werner Reutter. We are grateful to Thomas 227 Gramberg and Irmela Jeremias for providing reagents. We thank Sebastian Grothe, Yvonne 228 Voges, and Kerstin Lehr for technical assistance, and Alessia Ruggieri for graphical art work. 229 We are grateful to Richard Zehner for STR profiling. We acknowledge logistic support by 230 Nikolas Herold for LC-MS/MS analyses in the period 09-11/2014 as scientific staff in the 231 laboratory of O.T.K. at Goethe University. F.C. is supported by an EMBO long-term 232 fellowship (1305-2015 and Marie Curie Actions LTFCOFUND2013/GA-2013-609409). The 233 WEBs laboratory is supported by the Deutsche Forschungsgemeinschaft grant DFG EXC 234 1003 (H.S.). This work was supported in part by the Medical Faculty of the University of 235 Frankfurt (O.T.K.), Hilfe für krebskranke Kinder Frankfurt e.V. (J.C.), the Frankfurter 236 Stiftung für krebskranke Kinder (J.C.), by the LOEWE Program of the State of Hessia 237 (LOEWE Center for Translational Medicine and Pharmacology, Frankfurt)(G.G. and H.S.), 238 the José Carreras Leukämie-Stiftung (J.C.), the Deutsche Forschungsgemeinschaft (KE 742/4-239 1 (O.T.K.), SFB 1039/Z01 (G.G.)), the NSERC Strategic Network grant IBN (M.Mi.), the 240 Kent Cancer Trust (M.Mi.), and the LMU Munich (O.T.K.).

241

242 Author Contributions

J.C. and O.T.K. conceived the study and together with C.S., T.O., H.-M.B., and S.-M.S.
designed and analyzed the majority of experiments. D.T., R.F., H.B., L.S., M.Ma, and F.C.
conducted experiments, analyzed data, and provided discussion. A.C., J.L., M. Mi., and V.H.
provided critical reagents and discussion. G.G., M.-L.H., L.K., A.F.Y., P.S., N.F., C.S.,
W.E.B., W.H., E.W., and H.S. analyzed data and provided discussion. J.C. and O.T.K. wrote
and all authors edited the manuscript.

249 Competing Financial Interests Statement

- 250 The Johann Wolfgang Goethe-University has filed a patent application, on which several of
- the coauthors are listed as inventors.
- 252

253 **References**

- Lamba, J.K. Genetic factors influencing cytarabine therapy. *Pharmacogenomics* 10, 1657-1674 (2009).
 Burnett, A., Wetzler, M. & Lowenberg, B. Therapeutic advances in acute myeloid
- 256 2. Burnett, A., Wetzler, M. & Lowenberg, B. Therapeutic advances in acute myeloid
 leukemia. *J Clin Oncol* 29, 487-494 (2011).
- 258 3. Lowenberg, B., *et al.* Cytarabine dose for acute myeloid leukemia. *N Engl J Med* 364, 1027-1036 (2011).
- 4. Franzolin, E., *et al.* The deoxynucleotide triphosphohydrolase SAMHD1 is a major regulator of DNA precursor pools in mammalian cells. *Proc Natl Acad Sci U S A* 110, 14272-14277 (2013).
- Li, N., Zhang, W. & Cao, X. Identification of human homologue of mouse IFNgamma induced protein from human dendritic cells. *Immunol Lett* 74, 221-224 (2000).
- Kohnken, R., Kodigepalli, K.M. & Wu, L. Regulation of deoxynucleotide metabolism in cancer: novel mechanisms and therapeutic implications. *Mol Cancer* 14, 176 (2015).
 Hrecka, K., *et al.* Vpx relieves inhibition of HIV-1 infection of macrophages mediated
- 268 7. Hrecka, K., *et al.* Vpx relieves inhibition of HIV-1 infection of macrophages mediated
 269 by the SAMHD1 protein. *Nature* 474, 658-661 (2011).
- 270 8. Laguette, N., *et al.* SAMHD1 is the dendritic- and myeloid-cell-specific HIV-1
 271 restriction factor counteracted by Vpx. *Nature* 474, 654-657 (2011).
- 272 9. Dombret, H. & Gardin, C. An update of current treatments for adult acute myeloid
 273 leukemia. *Blood* 127, 53-61 (2016).
- 10. Crow, Y.J. & Rehwinkel, J. Aicardi-Goutieres syndrome and related phenotypes:
 linking nucleic acid metabolism with autoimmunity. *Hum Mol Genet* 18, R130-136 (2009).
- 277 11. Clifford, R., *et al.* SAMHD1 is mutated recurrently in chronic lymphocytic leukemia
 278 and is involved in response to DNA damage. *Blood* 123, 1021-1031 (2014).
- Merati, M., *et al.* Aggressive CD8(+) epidermotropic cutaneous T-cell lymphoma associated with homozygous mutation in SAMHD1. *JAAD Case Rep* 1, 227-229 (2015).
- Rentoft, M., *et al.* Heterozygous colon cancer-associated mutations of SAMHD1 have
 functional significance. *Proc Natl Acad Sci U S A* (2016).
- Lahouassa, H., *et al.* SAMHD1 restricts the replication of human immunodeficiency
 virus type 1 by depleting the intracellular pool of deoxynucleoside triphosphates. *Nat Immunol* 13, 223-228 (2012).
- 287 15. Baldauf, H.M., *et al.* SAMHD1 restricts HIV-1 infection in resting CD4(+) T cells.
 288 Nat Med 18, 1682-1687 (2012).

289	16.	Ballana, E., et al. SAMHD1 specifically affects the antiviral potency of thymidine
290		analog HIV reverse transcriptase inhibitors. Antimicrob Agents Chemother 58, 4804-
291		4813 (2014).
292	17.	Gramberg, T., Sunseri, N. & Landau, N.R. Evidence for an activation domain at the
293		amino terminus of simian immunodeficiency virus Vpx. J Virol 84, 1387-1396 (2010).
294	18.	Early, A.P., Preisler, H.D., Slocum, H. & Rustum, Y.M. A pilot study of high-dose 1-
295		beta-D-arabinofuranosylcytosine for acute leukemia and refractory lymphoma: clinical
296		response and pharmacology. Cancer Res 42, 1587-1594 (1982).
297	19.	Arnold, L.H., Kunzelmann, S., Webb, M.R. & Taylor, I.A. A continuous enzyme-
298		coupled assay for triphosphohydrolase activity of HIV-1 restriction factor SAMHD1.
299		Antimicrob Agents Chemother 59, 186-192 (2015).
300	20.	Huber, A.D., et al. SAMHD1 has differential impact on the efficacies of HIV
301		nucleoside reverse transcriptase inhibitors. Antimicrob Agents Chemother 58, 4915-
302		4919 (2014).
303	21.	Goldstone, D.C., et al. HIV-1 restriction factor SAMHD1 is a deoxynucleoside
304		triphosphate triphosphohydrolase. Nature 480, 379-382 (2011).
305	22.	Koharudin, L.M., et al. Structural basis of allosteric activation of sterile alpha motif
306		and histidine-aspartate domain-containing protein 1 (SAMHD1) by nucleoside
307		triphosphates. J Biol Chem 289, 32617-32627 (2014).
308	23.	Yan, J., et al. Tetramerization of SAMHD1 is required for biological activity and
309		inhibition of HIV infection. J Biol Chem 288, 10406-10417 (2013).
310	24.	Genome, C. Genomic and epigenomic landscapes of adult de novo acute myeloid
311		leukemia. N Engl J Med 368, 2059-2074 (2013).
312	25.	Komanduri, K.V. & Levine, R.L. Diagnosis and Therapy of Acute Myeloid Leukemia
313		in the Era of Molecular Risk Stratification. Annu Rev Med 67, 59-72 (2016).
314		

316

Figure 1 SAMHD1 expression levels inversely correlate with Ara-C cytotoxicity in 317 318 AML cell lines. (a) Representative immunoblots of SAMHD1 and other proteins previously 319 reported to be involved in Ara-C uptake and its conversion to the active Ara-C metabolite, 320 Ara-CTP, in the indicated AML cell lines. β -actin served as a loading control. Three 321 independent experiments were performed. Uncropped images are shown in **Supplementary** 322 **Figure 22**. (b-g) Correlation analyses between Ara-C IC_{50} values for these AML cell lines in a and the relative expression levels of SAMHD1 (b), ENT1 (c), DCK (d), CDA (e), DCTD 323 324 (f), or NT5C2 (g). Expression levels were normalized to β -actin and are shown as arbitrary 325 units (a.u.); the relative expression of each protein in THP-1 cells was set to 1. For **b-g**, closed 326 circles and error bars represent mean \pm s.e.m. of three independent experiments each 327 performed with technical replicates (n=3). Data in **b**-g were analysed using a linear regression model. R^2 values indicate goodness of fit of the regression model to the data, and represent 328 329 variance explained by the independent variable divided by total variance of the IC₅₀ Ara-C 330 values.

Figure 2 SAMHD1 counteracts Ara-C toxicity in AML cell lines via hydrolysis of the active metabolite, Ara-CTP. (a) Representative immunoblots for SAMHD1 after CRISPR/Cas9-mediated *SAMHD1* knockout in THP-1 (THP-1^{-/-}) cells or after shRNA or siRNA-mediated silencing of *SAMHD1* in OCI-AML3 and HEL cells. Alternatively, OCI-AML3 and MonoMac6 cells were transduced with VLPs carrying either lentiviral Vpr (Vpr-VLPs, control) or Vpx (Vpx-VLPs) proteins. β-actin served as a loading control. Uncropped images are shown in **Supplementary Figures 22** and **23**. (b) Ara-C IC₅₀ values of the

339	experimental groups shown in a. Each circle represents a technical replicate (n=3) of three
340	independent experiments performed. Horizontal lines and error bars represent means \pm s.e.m.
341	Numbers at the top indicate the factor of decrease of Ara-C IC ₅₀ values in SAMHD1-depleted
342	relative to control cells. (c) Ara-C IC_{50} values (top) and immunoblot for SAMHD1 (bottom)
343	in parental HEL cells or HEL cells stably transduced with either wildtype SAMHD1
344	(SAMHD1-WT) or the dNTPase-inactive D311A SAMHD1 mutant (SAMHD1-D311A). For
345	the IC_{50} data, the numbers above the bars indicate the factor by which the IC_{50} value differed
346	relative to HEL SAMHD1-WT cells. The IC ₅₀ values are shown as means \pm s.e.m. of three
347	independent experiments each performed with technical replicates (n=3) represented by
348	individual circles. β -actin served as a loading control for the SAMHD1 immunoblot.
349	Uncropped images are shown in Supplementary Figure 23. (d) Representative liquid
350	chromatography tandem mass spectrometry (LC-MS/MS) analysis of Ara-CTP in parental
351	HEL cells (blue chromatogram), HEL SAMHD1-WT cells (black chromatogram), or HEL
352	SAMHD1-D311A cells (red chromatogram). (e) HPLC analysis of products from an
353	enzymatic in vitro assay using bacterially expressed full-length SAMHD1. Ara-CTP was
354	incubated by itself (top), in the presence of SAMHD1 (middle), or in the presence of
355	SAMHD1 and the allosteric activator/substrate dGTP (bottom). Chromatogram peaks
356	corresponding to Ara-C, dG, and Ara-CTP are indicated. Statistical analyses were performed
357	using unpaired two-tailed Students' t-test. For (b) the degree of freedom was 16 and p<
358	0.0001 for all except for siRNA-treated HEL cells (df =4, p=0.0004). df was 16 and p<
359	

Figure 3 | SAMHD1 contributes to the acquired resistance of AML cells to Ara-C. (a) 363 364 Representative immunoblots of proteins involved in Ara-C uptake and metabolism in parental AML cell lines (HEL, HL-60, and Molm13) and in their respective Ara-C-resistant sublines 365 (HEL^rAra-C^{$2\mu g$}, HL-60^rAra-C^{$2\mu g$}, and Molm13^rAra-C^{$2\mu g$}). β -actin served as a loading control. 366 367 Three independent experiments were performed. Uncropped images are shown in 368 Supplementary Figure 24. (b) Quantitative analysis by LC-MS/MS of Ara-CTP levels in 369 parental and Ara-C-resistant AML cell lines. The means \pm s.d. of triplicates of one 370 representative experiment are shown; three independent experiments were performed. 371 Numbers above the bars represent the factor of decrease in Ara-CTP levels in Ara-C-resistant 372 cell lines relative to their parental counterparts. (c) Ara-C-resistant cell lines were treated with 373 the indicated VLPs and subsequently analyzed for Ara-C cytotoxicity (top) and SAMHD1 374 expression (bottom). Ara-C IC₅₀ values of three independent experiments each performed 375 with technical replicates (n=3) are presented with center lines showing the medians. The box 376 limits are quartiles 1 and 3, and whiskers show maximum and minimum values. Numbers above the bars indicate the factor of decrease in IC_{50} values in Vpx-VLP-treated cells relative 377 to Vpr-VLP-treated controls. (d) Representative LC-MS/MS chromatograms of Ara-CTP in 378 Molm13^rAra-C^{2µg} cells treated with either Vpr-VLPs (control, black), Vpx-VLPs (red), or left 379 380 untreated (blue). Statistical analyses were performed using unpaired two-tailed Students' t-381 test. For (b) the degree of freedom for all was 4 and exact p-values 0.0073 for HEL cells, 382 0.0037 for HL-60 cells and 0.0004 for Molm13 cells. df was 16 and p < 0.0001 for 383 (c).*p≤0.05; **p<0.01, ***p<0.001.

Figure 4 | SAMHD1 expression in leukemic blasts predicts response to Ara-C containing therapy in mouse transplantation models and AML patients. (a,b) Kaplan-

387 Meier survival analyses of Hoxa9/Meis1- (a) or MN1-driven (b) AML transplantation models using myeloid progenitors with endogenous SAMHD1 expression (SAMHD1^{+/+}) or 388 SAMHD1-deleted (SAMHD1^{-/-}) myeloid progenitors. Ara-C: i.p. administration of 75 mg/kg 389 390 Ara-C on days 18 and 19 after transplantation; Control: PBS. The difference in overall survival between Ara-C-treated SAMHD1^{+/+} and SAMHD1^{-/-} mice was statistically significant 391 (logrank test, Hoxa9/Meis1: p=2.97x10⁻⁶, n=10 both groups; MN1: p=2.97x10⁻⁶, n=10 both 392 groups). The differences between the two control groups and between SAMHD1^{+/+}Ara-C and 393 both control groups were not significant (Hoxa9/Meis1: p=0.42, SAMHD1^{-/-} (n=10) vs 394 SAMHD1^{+/+} (n=9); MN1: p=0.196, n=10 both groups). (c) Blasts isolated from bone marrow 395 396 from six adult AML patients (A-F) were transfected with SAMHD1-specific or control 397 siRNAs and two days later analyzed for Ara-C cytotoxicity (top) and SAMHD1 expression 398 (bottom). Ara-C IC₅₀ values are presented as the means \pm s.d. of the triplicates shown. The 399 numbers above the data points indicate the factor of difference between the siCTRL and 400 siSAMHD1 groups. Uncropped images are shown in Supplementary Figure 25. (d) 401 Representative IHC micrographs showing SAMHD1 and CD34 expression in bone marrow 402 (BM) from one No CR patient (#39), one CR patient (#28), and one healthy donor. Scale bar: 403 50 µm. (e) Comparison of SAMHD1 expression levels (IHC scores) in CR and No CR 404 patients. See Online Methods for an explanation of the IHC scores. Shown are relative 405 frequencies (in percent) of patients with IHC scores of 0, 1, 2 or 3 among CR (n=112) and No 406 CR (n=38) patients. f-h, Kaplan-Meier analyses for event-free survival (f), relapse-free 407 survival (g), and overall survival (h), for which AML patients were grouped into "No / low 408 SAMHD1 expressors" (IHC scores 0 or 1, red curves) versus "High SAMHD1 expressors" 409 (IHC scores 2 or 3, black curves). Numbers above the plots indicate the absolute number of 410 patients in each of the two groups at the respective time points. Significance of difference 411 between survival curves in **f**,**g**,**h** was assessed using the logrank test (p-values indicated in412 figure).

413

414 **ONLINE METHODS**

415 Ethics statement. Whole blood and bone marrow biopsies of AML patients were obtained 416 and collected pre- and post-treatment. All patients gave informed consent according to the 417 Declaration of Helsinki to participate in the collection of samples. The use of whole blood and 418 bone marrow aspirates was approved by the Ethics Committee of Frankfurt University 419 Hospital (approval no. SPO-01-2015) and University Hospital Münster (approval no. 2007-420 390-f-S).

421

422 **Plasmids.** The SIVmac251-based gag-pol expression constructs pSIV3+R- (Vpr-deficient) and pSIV3+X- (Vpx-deficient) were previously reported¹⁷. pLKO.1-puro-control-shRNA and 423 424 pLKO.1-puro-SAMHD1-shRNA#1-3 for shRNA-mediated silencing of SAMHD1 were previously described¹⁵. pHR-based transfer vectors expressing SAMHD1-WT or the D311A 425 426 mutant were generated by site-directed mutagenesis in a codon-optimized SAMHD1 427 expression construct (kindly provided by Dr. Thomas Gramberg, Institute of Clinical and 428 Molecular Virology, FAU Erlangen-Nürnberg, Erlangen, Germany) and subcloned into pHR-429 luc transfer vectors. pPAX2 was purchased from Addgene and pVSV-G has been previously described²⁶. 430

431

432 Cells and Reagents. Human AML cell lines including THP-1 (DSMZ no. ACC16; FAB M6),
433 OCI-AML2 (DSMZ No. ACC 99; FAB M4), OCI-AML3 (DSMZ No. ACC 582; FAB M4),
434 Molm13 (DSMZ No. ACC 554; FAB M5a), PL-21 (DSMZ No. ACC 536; FAB M3), HL-60

435 (DSMZ No. ACC 3; FAB M2), MV4-11 (DSMZ No. ACC 102; FAB M5), SIG-M5 (DSMZ 436 No. ACC 468; FAB M5a), ML2 (DSMZ No. ACC 15; FAB M4), NB4 (DSMZ No. ACC 437 207; FAB M3), KG1 (DSMZ No. ACC 14; FAB not indicated), MonoMac6 (DSMZ No. 438 ACC 124; FAB M5), and HEL (DSMZ No. ACC 11; FAB M6) were obtained from DSMZ 439 (Deutsche Sammlung von Mikroorganismen und Zellkulturen GmbH). All cell lines were 440 cultured in IMDM (Biochrom) supplemented with 10% FBS (SIG-M5 20% FBS), 4 mM L-441 Glutamine, 100 IU/ml penicillin, and 100 mg/ml streptomycin at 37°C in a humidified 5 % CO₂ incubator. Cells were routinely tested for mycoplasma contamination (LT07-710, Lonza) 442 and authenticated by short tandem repeat profiling, as reported²⁷. THP-1 cells deficient for 443 SAMHD1 (THP-1^{-/-}) and control cells (THP-1^{+/+}) were generated as previously described²⁸ 444 445 and cultivated in RPMI supplemented with 10% FCS, 100 IU/ml penicillin, and 100 mg/ml 446 streptomycin.

447 Mononuclear cells from blood or bone marrow AML samples were purified by Ficoll-Hypaque gradient centrifugation²⁶. Leukemic cells were enriched by negative selection with a 448 449 combination of CD3- (130-150-101), CD19- (130-150-301) and CD235a-microbeads (130-450 150-501, all from Miltenvi Biotec) according to the manufacturer's instructions and separated by the autoMACSTM Pro Separator. All preparations were evaluated for purity resulting in 451 452 >90% leukemic blasts. The AML-393 sample carrying a MLL-AF10 translocation was 453 derived from a 47 year old female with AML at relapse after bone marrow transplantation. 454 Primary cells were amplified in NSG mice and re-isolated from enlarged spleens as described²⁹. Frozen cells were kindly provided by Dr. Irmela Jeremias (Department of Gene 455 456 Vectors, Helmholtz Zentrum München, German Research Center for Environmental Health, 457 Munich, Germany) and thawed for experiments.

458 AML blasts (2 x 10^6) were cultivated in X-vivo 10 medium (Lonza) supplemented with 10%

459 HyClone FCS (Perbio), 4 mM L-glutamine, 25 ng/ml hTPO (130-094-013), 50 ng/ml hSCF

460 (130-096-695), 50 ng/ml hFlt3-Ligand (130-096-479) and 20 ng/ml hIL3 (130-095-069, all

461 from Miltenyi Biotec) in 96-well plates in the presence or absence of drugs.

The ecotropic GP+E86 packaging cell line was cultured in DMEM (Life Technologies) with 10% heat-inactivated FCS, 2 mM L-Glutamine, 100 U/ml Penicillin and 100 μ g/ml Streptomycin. Murine bone marrow cells were cultured in DMEM with 10% heat-inactivated FCS, 2 mM L-Glutamine, 100 U/ml Penicillin and 100 μ g/ml Streptomycin supplemented with 10ng/ml murine recombinant IL3 (213-13), 10 ng/ml human recombinant IL6 (200-06), and 100ng/ml murine recombinant SCF (250-03) (all from Peprotech).

Ara-C was purchased from Tocris (147-94-4), daunorubicin from Selleckchem (S3035), etoposide from TEVA (45891.00), fludarabine from Tocris (21679-14-1) and dFdC (gemcitabine) from Accord Healthcare GmbH (82092.00.00). Deoxynucleosides (dNs) (Sigma-Aldrich), which are dNTP precursors, were used as previously reported¹⁵. All nucleotide standards and internal standards for the LC-MS/MS analysis were obtained from Sigma-Aldrich, Silantes or Alsachim³⁰. Labeled cytarabine, ¹³C₃-Ara-C (SC-217994, Santa Cruz), was used for LC-MS/MS analysis.

475

476 Generation of Ara-C-resistant cell lines. Ara-C-resistant cell lines were established by continuous exposure of Ara-C sensitive cell lines HL-60, HEL, Molm13, THP-1, MV4-11, 477 OCI-AML3 to increasing drug concentrations as previously described^{31,32} and are part of the 478 479 Resistant Cancer Cell Line (RCCL) collection 480 (http://www.kent.ac.uk/stms/cmp/RCCL/RCCLabout). Briefly, cells were cultured at 481 increasing Ara-C concentrations starting with concentrations that inhibited viability of the parental cell lines by 50 % (IC₅₀). Ara-C concentrations were doubled every 2 to 6 weeks until cells readily grew in the presence of 2 μ g Ara-C. Resistant cell lines were designated as HL-60^rAra-C^{2 μ g}, HEL^rAra-C^{2 μ g}, Molm13^rAra-C^{2 μ g}, THP-1^rAra-C^{2 μ g}, MV4-11^rAra-C^{2 μ g} and OCI-AML3^rAra-C^{2 μ g} and were continuously cultured in the presence of 2 μ g Ara-C. Cells were routinely tested for mycoplasma contamination (LT07-710, Lonza) and authenticated by short tandem repeat profiling²⁷.

488

489 **Cell viability assay.** The viability of AML cell lines treated with various drug concentrations 490 was determined by the 3-(4,5-dimethylthiazol-2-yl)-2,5-diphenyltetrazolium bromide (MTT) 491 dye reduction assay after 96 hours of incubation as described previously³³. IC_{50} values were 492 determined using CalcuSyn (Biosoft).

493

494 **Cytotoxic assay for AML blasts** *ex vivo*. The cell viability of AML blasts was determined 495 after 96 hours of incubation by the quantification of ATP levels in cell culture supernatants 496 using the CellTiter-Glo[®] Luminescent Cell Viability Assay (G7573, Promega) according to 497 the manufacturer's instructions. Luminescence was measured on a Tecan infinite M200 498 (TECAN) instrument at a wavelength of 560 nm (reference wavelength 620 nm). IC₅₀ values 499 were determined using CalcuSyn (Biosoft).

500

501 **Apoptosis assays.** Sub-G1 cells as a marker for DNA fragmentation in late apoptotic cells 502 were measured according to Nicoletti by flow cytometry³⁴. Briefly, Ara-C-treated and 503 untreated cells were washed once in 1x PBS, incubated for at least 2h at 4°C with Nicoletti 504 buffer (0.1 % trisodiumcitrate-dihydrate pH 7.4, 0.1% Triton X-100, 50 μ g/ml propidium 505 iodide), and diluted prior to measurement in 1x PBS. Samples were analyzed using a 506 FACSVerse (BD Biosciences) and FlowJo software (TreeStar). Alternatively, Caspase 3/7 507 activity as a surrogate for early apoptosis was quantified by luminescence. Briefly, Ara-C-508 treated and untreated cells were measured using the Caspase-Glo[®] 3/7 assay (G8091, 509 Promega) according to the manufacturer's instructions. Luminescence was measured on a 510 Tecan infinite M200 (TECAN) instrument at a wavelength of 560 nm (reference wavelength 511 620 nm).

512

Flow cytometry. Intracellular SAMHD1 staining was performed as previously described¹⁵. Staining for surface markers (CD33, CD34, CD45) was applied prior to fixation. The following fluorochrome-conjugated antibodies were used: CD33-PE (130-091-732), CD34-FITC (130-081-001, both from Miltenyi Biotech), and CD45-V450 (560373, BD Pharmingen), all diluted 1:11 per 10⁷ cells, and Alexa-Fluor-660 (A-21074, Invitrogen, Life technologies, 1:200). Samples were analyzed using a FACSVerse or FACSCanto II flow cytometer (BD Biosciences) and FlowJo software (TreeStar).

520 For *in vitro* characterization of Hoxa9/Meis1- and MN1-transformed myeloid progenitor cells. 521 surface-marker expression was characterized by flow cytometry using a LSRFortessa flow cytometer (BD Biosciences). Briefly, cells $(2x10^5)$ were washed twice with 2% FCS in PBS 522 523 and stained with the following antibodies: PerCP-Cy5.5-conjugated anti-mouse Gr1 (45-524 5931), V450-conjugated anti-mouse Mac1 (48-0112), APC-conjugated anti-mouse c-kit (17-525 1171), PE-Cy7-conjugated anti-mouse Sca1 (25-5981), PE-conjugated anti-mouse FceRI (12-526 5898, all from eBioscience), and APC-H7-conjugated anti-mouse CD19 (560245, BD 527 Bioscience). 7-AAD (BD-Bioscience) was used for exclusion of dead cells.

529 **Immunoblotting.** Cells were lysed in Triton X-100 sample buffer and proteins separated by sodium dodecyl sulfate-polyacrylamide gel electrophoresis. Proteins were blotted onto a 530 531 nitrocellulose membrane (Thermo Scientific). The following primary antibodies were used at 532 the indicated dilutions, SAMHD1 (12586-1-AP, Proteintech, 1:1000), β-actin (3598R-100, 533 BioVision via BioCat, 1:2000), DCK (sc-393099, Santa Cruz, 1:500), CDA (sc-365292, Santa Cruz, 1:100), ENT1 (ab135756, Abcam, 1:500), and NT5C2 (H00022978-M02, Abnova, 534 1:200), DCTD (NBP1-75825, Novus, 1:200). Visualization and quantification was performed 535 using fluorescently labeled secondary antibodies (926-32210 IRDve® 800CW Goat anti-536 Mouse and 926-32211 IRDve[®] 800CW Goat anti-Rabbit, LI-COR, 1:20000) and an Odvssev 537 538 CLx Imaging system (LI-COR Biosciences).

539

540 Patients. Patients were admitted to the University Hospital Frankfurt between 2010 and 2014 541 and treated for newly diagnosed AML with regimens containing standard dose Ara-C and daunorubicin ("7+3") (83 patients) or Ara-C alone (1 patient) (Supplementary Table 6); an 542 543 additional 66 patients admitted to the University Hospital Münster were included in the IHC 544 analyses. In addition, viable AML cells were purified from bone marrow of patients that were 545 admitted to the University Hospital Frankfurt in 2015 and 2016 (Supplementary Table 3). 546 Patients at the University Hospitals of Frankfurt and Münster are routinely advised to undergo 547 a bone marrow biopsy at diagnosis. All patients consented to the scientific analyses of their 548 data and to scientific analyses of biomaterial that was obtained for diagnostic purposes. All patients received at least one course of Ara-C at a dose of 100 mg/m² over 7 days and 549 daunorubicin at a dose of 60 mg/m^2 over 3 days ("7+3") (if not otherwise stated). All patients 550 551 below the age of 60 received a second cycle of induction therapy. Patients over the age of 60 552 received a second induction cycle only if their day 15 bone marrow aspirate showed more than 5% blasts. For the analyses, patient records were reviewed by physicians who were unaware of the SAMHD1 expression results in the diagnostic biopsies. Remission criteria and cytogenetic risk groups were assessed according to the ELN guidelines.

The initial response to induction therapy was analyzed in bone marrow biopsies/aspirates and defined as complete (CR) if the blast count was <5%, and as "No CR" if the blast count was >5%. For the calculation of event-free survival (EFS), events were defined as failure to achieve complete remission (CR, CRi, CRp) within 40 days after the last induction cycle, relapse, or death at any time after start of therapy. Relapse-free survival (RFS) and remission duration were calculated only in patients that achieved CR.

562

563 **Immunostaining of bone marrow samples.** Bone marrow samples from 154 patients, 564 including 150 AML patients and four healthy donors, were provided by the University 565 Hospital Frankfurt and University Hospital Münster, Germany. Tissues were fixed in 4% 566 buffered formalin, descaled by EDTA and embedded in paraffin. Immunohistochemical staining was performed as previously described³⁵. Briefly, 2- μ m bone marrow tissue sections 567 568 were incubated with EnVision Flex Target Retrieval Solution, pH low (K8005, DAKO) and 569 stained with primary antibodies directed against SAMHD1 (12586-1-AP, Proteintech, 1:3000) 570 and against CD34 (IR632, DAKO) for 40 min at room temperature. Polymeric secondary 571 antibodies coupled to HRPO peroxidase and DAB were used for visualization (REAL 572 EnVision Peroxidase/DAB+, K5007, DAKO). Tissue samples were analyzed by light 573 microscopy after counterstaining with Meyer's haematoxylin (K8008, DAKO).

574 Two pathologists, who were blinded to clinical history and therapeutic response, 575 independently scored the SAMHD1 IHCs. They evaluated all tissue sections for nuclear 576 SAMHD1 staining using a four-stage staining score: 0 = negative, 1 = weak intensity of staining, 2 = strong intensity of staining in less than 25% of blasts, 3 = strong intensity of
staining in more than 25% of blasts. IHC staining scores of 0 and 1 were defined as "No / low
expression" and IHC staining scores of 2 and 3 were defined as "High SAMHD1 expression".
Membranous CD34 staining for the quantification of the number of AML blasts was
evaluated using a two-stage staining score: 0 = negative, 1 = positive.

582

583 Retrospective analysis of the TCGA AML cohort. Clinical data, mutational profiles and 584 normalized gene expression data for a cohort of 200 AML patients from The Cancer Genome Atlas (TCGA, run date 20150821)²⁴ were retrieved using the RTCGA-Toolbox 585 R/BioConductor package, version 2.2.2³⁶. All analyses were performed using R 3.3.0 and 586 587 custom scripts. To test the association between SAMHD1 expression and first complete 588 remission, all Ara-C-treated patients with available gene expression data were considered. To 589 test the association between SAMHD1 expression and cytogenetic risk, all patients with 590 available gene expression data were considered. For analysis of mutation rates, all patients 591 with available mutational profiles were considered.

592

593 Mice and retroviral infection of lineage-depleted bone-marrow cells. C57BL/6J female 594 mice (age: 8-12 weeks) were obtained from Janvier-Labs (Le Genest-Saint-Isle, France). All 595 animal experiments were performed according to the regulations of the United Kingdom 596 Home Office and German authorities. All animal experiments were performed according to 597 national and international standards. Bone marrow cells were harvested from mice, and 598 lineage-negative cells were obtained by negative selection using the Lineage Cell Depletion 599 Kit (130-090-858, Miltenvi Biotec) as recommended by the manufacturer. Lineage-negative 600 cells were co-cultured with GP+E86 cells packaging MSCV-Hoxa9-PGK-neo in the presence

601 of polybrene (10 µg/ml, Sigma-Aldrich) for 3 days followed by co-incubation with GP+E86 602 MSCV-Meis1-IRES-YFP for 1 day. Hoxa9-expressing cells were selected with 0.6 mg/ml 603 G418 (Sigma-Aldrich) for at least 5 days. MN1-overexpressing myeloid progenitor cells were 604 generated as described previously³⁷. After selection, cells were sorted with a FACS BD Aria 605 III cell sorter. Lentiviral transductions of cultured cells with pLentiCRISPRv2 vectors 606 encoding SAMHD1-specific CRISPR or control vectors were performed as described previously³⁵ using BU033 (5' CACCGgacgatcctcatccaaaaa 3') and BU034 (5' 607 608 AAACtttttggatgaggatcgtcC 3') (Fig. 4a,b), or BU035 (5' CACCGgatgattctgataaggaga 3') and 609 BU036 (5' AAACtctccttatcagaatcatcC 3') (Supplementary Fig. 14).

610

611 **Transplantation and monitoring analyses of transplanted mice.** 7.5×10^4 cells were 612 transplanted together with 2×10^5 "support cells" by injection into the tail vein of lethally 613 irradiated (9.5 Gy) recipient mice (C57BL/6J). Wild-type mononuclear bone marrow cells 614 isolated from C57BL/6J mice and purified on a Ficoll gradient (Sigma-Aldrich) were used as 615 support cells to reconstitute hematopoiesis in irradiated recipient mice. 18 days after 616 transplantation, mice were treated with 75 mg/kg cytarabine or PBS (i.p.) for 2 subsequent 617 days.

Blood and bone marrow cells were isolated from mice for further analyses. Blood counts were analyzed with ScilVet abc animal blood cell counter (Scil Animal Care Company). Cells from spleen and bone marrow were incubated for 10 min with erythrocyte lysis buffer (155 mM NH₄Cl, 10 mM KHCO₃, 0.1 mM EDTA) and then washed twice with 2% FCS in PBS. Staining was performed as described above.

Blood smears and purified cells from bone marrow and spleen were centrifuged on cover slips $(2x10^5 \text{ cells/slip})$. Subsequently, cells were fixed for 10 min with methanol and stained with a

May-Grünwald solution for 8 min followed by Giemsa (both Merck Millipore) staining for 20min.

627

mRNA analyses. RNA extraction and TaqMan-based mRNA quantification of SAMHD1
(Applied Biosystems: assay no. Hs00210019-m1) and RNaseP (Applied Biosystems:
TaqMan® RNase P Control Reagents Kit (4316844), endogenous reference control) were
performed essentially as reported³⁸.

632

LC-MS/MS analysis. Cells (5 x 10^5) were treated with 10 µg/ml $^{13}C_3$ -Ara-C (SC-217994, 633 634 Santa Cruz) and incubated at 37° C in a humidified 5 % CO₂ incubator for 6 h. Subsequently, 635 cells were washed twice in 1 ml PBS, pelleted and stored at -20°C until measurement. The concentrations of dNTPs, ¹³C₃-Ara-CTP, and dFdC-TP in the samples were analyzed by 636 liquid chromatography-electrospray ionization-tandem mass spectrometry essentially as 637 previously described³⁰. Briefly, the analytes were extracted by protein precipitation with 638 639 methanol. An anion exchange HPLC column (BioBasic AX, 150 x 2.1 mm, Thermo) was 640 used for the chromatographic separation and a 5500 QTrap (Sciex) instrument was used to 641 analyze the samples, operating as triple quadrupole in positive multiple reaction monitoring (MRM) mode. Analysis of dNTPs was performed as previously described³⁰. Additionally, 642 ¹³C₃-Ara-CTP and dFdC-TP were quantified using Cytidine-¹³C₉, ¹⁵N₃-5'-triphosphate as an 643 644 internal standard (IS). The precursor-to-product ion transitions used as quantifiers were m/z $487.0 \rightarrow 115.1$ for ${}^{13}C_3$ -Ara-CTP and m/z 504 $\rightarrow 326$ for dFd-CTP. Due to the lack of 645 commercially available standards of ¹³C₃-Ara-CTP and dFd-CTP, relative quantification was 646 647 performed by comparing the peak area ratios (analyte/IS) of the differently treated samples.

Production of lentiviral expression vectors and VLPs. Lentiviral vectors expressing SAMHD1-WT or SAMHD1-D311A were generated by co-transfection of packaging vector pPAX2, either pHR-SAMHD1-WT or pHR-SAMHD1-D311A and a plasmid encoding VSV-G. VLPs, carrying either Vpx or Vpr from SIVmac251, were produced by co-transfection of 293T cells with pSIV3+ *gag pol* expression plasmids and a plasmid encoding VSV-G. The SAMHD1 degradation capacity of Vpx-VLPs was determined in THP-1 cells 24 h post transduction by intracellular SAMHD1 staining.

656

657 Manipulation of intracellular SAMHD1 levels. For shRNA-mediated silencing of 658 SAMHD1, OCI-AML3 cells were transduced by spinoculation with VSV-G pseudotyped 659 lentiviral vectors carrying either pLKO.1-puro-control-shRNA or pLKO.1-puro-SAMHD1-660 shRNA#1-3. On day 10 after transduction, successfully transduced cells were selected with 661 puromycin (P8833, Sigma-Aldrich) (7.5 µg/ml). SAMHD1 levels were monitored by 662 intracellular SAMHD1 staining and Western blotting. For siRNA-mediated silencing, AML cells (1.2 x 10^6) were transfected with 2.5 µM ON-TARGET plus human SAMHD1 siRNA 663 664 SMART-pool (L-013950-01-0050, Dharmacon) in resuspension electroporation buffer R 665 (Invitrogen) using the Neon transfection system (Invitrogen). Additionally, ON-TARGET 666 plus Non-targeting Pool (D-001810-10-50, Dharmacon) was transfected in parallel. 667 Electroporation was performed using one 20 msec pulse of 1700 V and analyzed 48 h post-668 transfection via Western blotting and cell viability assay. The following siRNA duplexes were 669 used: non-targeting (UGGUUUACAUGUCGACUAA;UGGUUUACAUGUUGUGUGA; 670 UGGUUUACAUGUUUUCUGA; UGGUUUACAUGUUUUCCUA), 671 SAMHD1 (GACAAUGAGUUGCGUAUUU; CAUGUUUGAUGGACGAUUU:

672 AAGUAUUGCUAGACGUGAA; UUAGUUAUAUCCAGCGAUU).

HEL cells were transduced by spinoculation with VSV-G pseudotyped lentiviral vectors
carrying either SAMHD1-WT or the D311A mutant. Expression of SAMHD1 was monitored
by intracellular SAMHD1 staining and Western blotting. AML cell lines and primary AML
blasts were spinoculated with VSV-G pseudotyped VLPs carrying either Vpx or Vpr.

677

678 HPLC assays for hydrolysis. To investigate whether or not Ara-CTP or dFd-CTP are hydrolyzed by SAMHD1, HPLC assays were performed as described previously³⁹. The 679 680 reaction mixtures (50 µl) contained 50 mM Tris-HCl (pH 7.5), 10 mM MgCl₂, 100 mM NaCl, 681 1 mM DTT, 1 mM Ara-CTP or dFdCTP, 0.2 mM activator (dGTP), and SAMHD1 (4 µM). In 682 some experiments, the SAMHD1 substrate TTP was used as positive control. Reaction 683 mixtures were incubated at 37°C and passed through 10K VWR Centrifugal Filters to quench 684 the reactions and remove the protein. Reaction products were analyzed by ion-pair reverse-685 phase HPLC using a Varian Pursuit C18 column (150 × 4.6 mm) in a Varian ProStar HPLC 686 system with a photodiode array detector set at 260 nm. The mobile phase for separation of 687 nucleotides consisted eluants: 0.1 mM KH₂PO₄ (pH 6.0)with 8 of two 688 mM tetrabutylammonium hydroxide 0.1 mM KH₂PO₄ (pH 6.0) with 8 and 689 mM tetrabutylammonium hydroxide and 30 % methanol.

690

691 **Statistical analysis.** Statistical data analysis was performed using GraphPad Prism. Linear 692 regression and nonlinear fitting using one phase decay was used to assess correlation of 693 protein expression, mRNA levels, or IC_{50} values (**Fig. 1, Supplementary Figs. 2,3,15,17**). R² 694 were used to assess the quality of the fit. Unpaired group comparisons were performed using 695 Student's *t*-test. In **Supplementary Fig. 11**, paired group comparisons were performed using 696 Student's *t*-test. F-test was used to assess significance of regression models (**Supplementary**

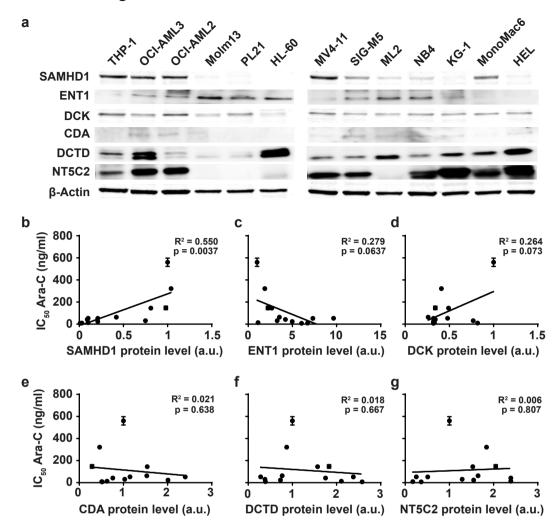
697	Fig. 3)	. Comparisons of multiple groups were performed using 1-way ANOVA. Statistical			
698	data	analysis of AML patient data was performed in R version 3.2.5			
699	(R Core Team, 2016, <u>https://www.R-project.org/)</u> , using Kaplan-Meier analysis and logrank				
700	test for survival analysis.				
701					
702	Data availability				
703	The C	ancer Genome Atlas data (TCGA) can be retrieved using the RTCGA-Toolbox			
704	R/Bio(Conductor package, version 2.2.2. Plasmids are available upon request.			
705					
706					
707	26.	Keppler, O.T., et al. Susceptibility of rat-derived cells to replication by human			
708		immunodeficiency virus type 1. J Virol 75, 8063-8073 (2001).			
709	27.	Capes-Davis, A., et al. Match criteria for human cell line authentication: where do we			
710		draw the line? Int J Cancer 132, 2510-2519 (2013).			
711	28.	Wittmann, S., et al. Phosphorylation of murine SAMHD1 regulates its antiretroviral			
712		activity. <i>Retrovirology</i> 12 , 103 (2015).			
713	29.	Vick, B., et al. An advanced preclinical mouse model for acute myeloid leukemia			
714		using patients' cells of various genetic subgroups and in vivo bioluminescence			
715		imaging. PLoS One 10, e0120925 (2015).			
716	30.	Thomas, D., Herold, N., Keppler, O.T., Geisslinger, G. & Ferreiros, N. Quantitation of			
717		endogenous nucleoside triphosphates and nucleosides in human cells by liquid			
718		chromatography tandem mass spectrometry. <i>Anal Bioanal Chem</i> 407 , 3693-3704			
719	21	(2015).			
720	31.	Kotchetkov, R., <i>et al.</i> Increased malignant behavior in neuroblastoma cells with			
721		acquired multi-drug resistance does not depend on P-gp expression. <i>Int J Oncol</i> 27,			
722	22	1029-1037 (2005). Michaelie M., et al. A dentation of company cells from different artitics to the MDM2			
723	32.	Michaelis, M., <i>et al.</i> Adaptation of cancer cells from different entities to the MDM2 inhibitor puttin 2 people in the emergence of π 52 mutated multi-days period entry.			
724		inhibitor nutlin-3 results in the emergence of p53-mutated multi-drug-resistant cancer			
725 726	33.	cells. <i>Cell Death Dis</i> 2 , e243 (2011). Michaelis, M., <i>et al.</i> Identification of flubendazole as potential anti-neuroblastoma			
720	55.	compound in a large cell line screen. <i>Sci Rep</i> 5 , 8202 (2015).			
728	34.	Riccardi, C. & Nicoletti, I. Analysis of apoptosis by propidium iodide staining and			
728	J 1 .	flow cytometry. <i>Nat Protoc</i> 1 , 1458-1461 (2006).			
730	35.	Oellerich, T., <i>et al.</i> FLT3-ITD and TLR9 use Bruton tyrosine kinase to activate			
730	55.	distinct transcriptional programs mediating AML cell survival and proliferation. <i>Blood</i>			
732		125 , 1936-1947 (2015).			
733	36.	Samur, M.K. RTCGAToolbox: a new tool for exporting TCGA Firehose data. <i>PLoS</i>			
734	50.	<i>One</i> 9 , e106397 (2014).			

735 37. Heuser, M., et al. MN1 overexpression induces acute myeloid leukemia in mice and 736 predicts ATRA resistance in patients with AML. Blood 110, 1639-1647 (2007). 737 Goffinet, C., Schmidt, S., Kern, C., Oberbremer, L. & Keppler, O.T. Endogenous 38. 738 CD317/Tetherin limits replication of HIV-1 and murine leukemia virus in rodent cells 739 and is resistant to antagonists from primate viruses. J Virol 84, 11374-11384 (2010). 740 39. Beloglazova, N., et al. Nuclease activity of the human SAMHD1 protein implicated in the Aicardi-Goutieres syndrome and HIV-1 restriction. J Biol Chem 288, 8101-8110 741 742 (2013)743

744 Editorial summary

- 745 The therapeutic response of acute myeloid leukemia to the nucleoside analog Ara-C is
- regulated by SAMHD1, an enzyme which is differentially expressed in this cancer and which
- 747 hydrolyzes the active metabolite Ara-CTP.
- 748
- 749

Schneider et al., Figure 1



Schneider et al., Figure 2

